RSC Advances

PAPER

View Article Online
View Journal | View Issue

Cite this: *RSC Adv.*, 2019, **9**, 27583

Visual artificial tongue for identification of various metal ions in mixtures and real water samples: a colorimetric sensor array using off-the-shelf dyes†

Yuanfang Huang,[ab] Peiwen Cheng[c] and Chunyan Tan *[ab]

Received 1st August 2019
Accepted 23rd August 2019

DOI: 10.1039/c9ra05983k

rsc.li/rsc-advances

A three-unit colorimetric sensor array in aim of detecting heavy metal ions has been constructed with two off-the-shelf dyes. Multivariate data analysis is performed using LDA and HCA to recognize colour change patterns based on both absorption spectra and RGB values from image scans. The sensor array is able to differentiate 15 metal ions not only in separate solutions, but also mixtures of 3, 5, and 7 different metal ions and real water samples.

Pollution of heavy metal ions in water and soil has become a worldwide environmental concern, due to their great harm to animal and human health even at low concentrations. Hence, to identify and distinguish heavy metal ions both qualitatively and quantitatively has been a field of constant research interest. Traditional methods for heavy metal ion detection such as inductively coupled plasma mass spectrometry (ICP-MS) and atomic absorption spectroscopy (AAS) are, although accurate and most common, very unpractical for on-site testing. A more convenient technique is continuously under demand.

Inspired by mammalian olfactory and gustatory systems, array-based sensing platforms, which use a series of cross-reactive sensors instead of specific probes, have emerged as promising alternatives due to their simple fabrication, flexibility, convenient data collection and analysis. Sensor arrays have been reported to distinguish combinations of many analytes and mixtures,[1,2] including physical stimuli (temperature, humidity, light), volatile organic compounds, explosives, toxic industrial chemicals, metal ions, flavonoids, biomolecules (biothiols, phosphates), pesticides, proteins, pathogens (virus, bacteria, fungi), cells, food and beverages (liquors, teas, milks, red wines, coffees, whiskies), herbal medicines, and disease biomarkers.[3–7]

For metal ions discrimination and quantification, there are different analytical methods to construct response patterns, including electrochemical methods,[8] steady-state and time-resolved fluorescence spectroscopy,[9–14] UV-visible absorption spectroscopy,[15,16] and digital imaging and colour calibration.[17–21] Although most reported work successfully distinguished samples of single metal ions or mixtures of up to 3 metal ions, applicable methods for analysis of mixtures consisting of more than 3 metal ions as well as real water samples are still of great challenge.

Herein, we developed a simple and cost-effective three-unit colorimetric sensor array (Scheme 1) using dithizone in two solvent conditions and resazurin (structures shown in Fig. 1), to distinguish 15 different metal ions, their mixtures, as well as real water samples. Pattern recognition based on data from absorption spectra as well as scanned-images was realized using linear discriminant analysis (LDA) and hierarchical clustering analysis (HCA).

Dithizone was reported to show different colour responses towards diverse metal ions, including Co^{2+}, Ni^{2+}, Cu^{2+}, Zn^{2+}, Mn^{2+} Ag^{+}, Cd^{2+}, and Hg^{2+}.[22–24] Yet its application as a practical sensing molecule for metal ions is limited by its poor solubility in aqueous solution. CTAB was found to improve dithizone's sensitivity for metal ions detection by favouring dissolution and

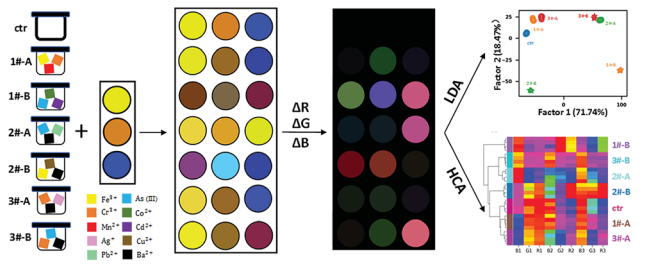

Scheme 1 Schematic illustration of colorimetric sensor array for detection of metal ions.

[a]*Open FIESTA, Tsinghua Shenzhen International Graduate School, Tsinghua University, Shenzhen, P. R. China, 518055*

[b]*State Key Laboratory of Chemical Oncogenomic, Tsinghua Shenzhen International Graduate School, Tsinghua University, Shenzhen, P. R. China, 518055. E-mail: tancy@sz.tsinghua.edu.cn; Fax: +86-755-26032094; Tel: +86-755-26036533*

[c]*Shenzhen College of International Education, Shenzhen, P. R. China, 518048*

† Electronic supplementary information (ESI) available. See DOI: 10.1039/c9ra05983k

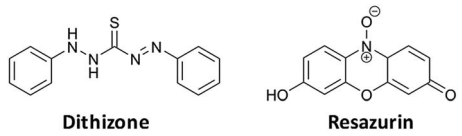

Fig. 1 Structures of the two off-the-shelf dyes used in our sensor array.

interaction of dithizone with metal ions.[25,26] Moreover, the pH value of the solution was also reported to influence the property of dithizone, which causes distinct absorption spectral change and colour alteration.[27] Thus, we introduced NaOH to the second unit to generate multidimensional information. These different solvent conditions were screened with varying amounts of the surfactant CTAB and NaOH in HEPES for the optimization of dithizone sensing. Based on the results of preliminary experiments (Fig. S1†), dithizone/CTAB (unit 1: 30 μM of dithizone and 90 μM of CTAB in HEPES buffer) and dithizone/CTAB/NaOH (unit 2: 30 μM of dithizone, 10 mM of CTAB, and 6 mM of NaOH in HEPES buffer) were used as two sensor units in the array. Resazurin was reported capable of discriminating different metal ions based on its voltammetric behaviour.[28] Thus we also included it in our sensor array as unit 3 (unit 3: 24.5 μM of resazurin in water).

To test the proof-of-concept of the proposed three-unit sensor array, 15 metal ions (Pb^{2+}, Ag^{+}, Cr^{3+}, Cd^{2+}, Fe^{3+}, As(III), Zn^{2+}, Ni^{2+}, Cu^{2+}, Mn^{2+}, Ba^{2+}, Al^{2+}, Co^{2+}, Sn^{2+}, Hg^{2+}, each at 5 μM), were selected as analytes. In our study, data were acquired by two different methods, using microplate reader to generate absorption spectral measurement, as well as using flatbed scanner to obtain RGB values in images. Compared to common colorimetric methods which require complex instrumentation, the latter method above demonstrated its convenience by its simple operation, straightforward visualization effect, and good sensitivity. Firstly, the real digital images of the three-unit sensor array upon adding single metal ions at the concentration of 5 μM were recorded by a commercially available and cheap flatbed scanner (Fig. 2A). For each well on the plate, the red, green, and blue (RGB) values from the centre were extracted using our program written in Python (version 3.7.3). The changes of RGB values with and without metal ions, ΔR, ΔG, and ΔB, were used to generate the false-colour images (Fig. 2B) and the corresponding heat map (Fig. 2C). Obvious colour change can be seen in the presence of Ni^{2+}, As(III), Hg^{2+}, Co^{2+}, Cu^{2+}, Zn^{2+}, Fe^{3+}, Cr^{3+}, while only subtle changes take place in the presence of Sn^{2+}, Al^{3+}, Cd^{2+}, Ba^{2+}. These different responses presumably result from the different interactions between the sensor units and metal ions.

LDA was then applied to further digitize and visualize the colour change patterns. LDA is a statistical analysis method that can visually differentiate two or more kinds of objects or events based on their linear combination of features, selected so as to maximize the ratio of inter-class variance to intra-class variance. All metal ions at the concentration of 5 μM were tested using four replicate measurements to provide a training matrix of sixteen samples (fifteen metal ions + one control) × three

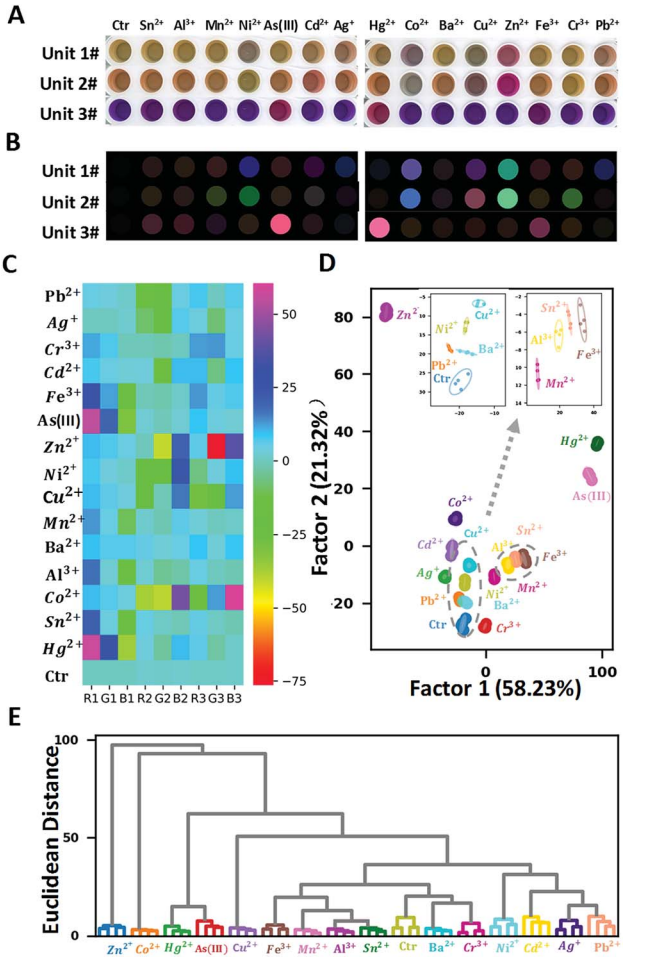

Fig. 2 Performance of sensor array to 15 metal ions single solutions based on colour image change pattern (A) colour image of sensor array recorded by flatbed scanner upon addition of metal ions. (B) Colour difference map of the sensor array. For purposes of visualization, the colour range of the difference map was expanded from 4 to 8 bits per colour (RGB range of 0–58 expanded to 0–255). (C) Heatmap derived from the difference map. (D) LDA 2D plot and (E) HCA dendrogram derived from the colour response pattern of sensor array. Concentration of all used metal ions is 5 μM.

sensors × three colour channels × four replicates. The resulting training data were analysed and processed through LDA using Sci-kit learn package (version 0.21.2) in Python and transformed into nine canonical scores, which account for 58.23%, 21.32%, 15.40%, 3.53%, 0.82%, 0.38%, 0.16%, 0.10%, 0.04% of variations, respectively. The first two factors accounted for 79.55% of the total variance and were used to construct the two-dimensional (2-D) discrimination plot (Fig. 2D). All the metal ions can be separately grouped with clarity, despite the relatively close between clusters of Al^{3+}, Sn^{2+}, Fe^{3+} and the high proximity between clusters of Pb^{2+} and Ba^{2+} (as shown in the magnified inset of Fig. 2D).

HCA is a common method to build a hierarchy of clusters according to their similarity characterized by the Euclidean distance. Unlike LDA, in which only a few most significant factors are used to do the visualization (in this case, the first

three factors accounted for the 91.12% variance of the total), HCA takes all the features into consideration when computing the Euclidean distance among samples. As shown in Fig. 2E, HCA resulted in clear discrimination of 15 metal ions and the control with no misclassification, confirming that the proposed sensor array has strong discrimination ability of these 15 metal ions.

Then "leave-one-out" cross-validation was used to evaluate the prediction ability of the LDA classifier. The training set was prepared by removing each sample one at a time, and the LDA model was built on the "leave-one-out" training set. Then the removed sample was reclassified using the LDA model. According to the classification result, the percentage of correct classification by the LDA model would be calculated. In this study, leave-one-out cross-validation for the LDA classification mode showed 100% accuracy for prediction of 15 metal ions at the concentration of 5 μM.

As a comparison, UV-vis absorption spectra of the array upon adding these metal ions at the same concentrations were measured using a microplate reader and the response patterns were analysed as well. The patterns of the absorbance change were obtained as $(A_0 - A)/A_0$, in which A_0 and A are the absorbance without and with metal ions, respectively, in the following equation in specific wavelength range for each sensor unit. As shown in Fig. S2,† three units responded differently to addition of different metal ions. In order to maximize the spectral information as well as minimize the influence of noise, 61 wavelengths (350–650 nm, every 5 nm) of the first unit, and 55 wavelengths (350–620 nm, every 5 nm) of the other two units were selected for further analysis respectively. Similarly, LDA, "leave-one-out" cross validation, and HCA were applied to characterize the absorbance change patterns. All samples were completely separated into different clusters (Fig. S3†), including the clusters of Pb^{2+} and Ba^{2+}, which were in high proximity in the RGB data analysis. The improved classification performance presumably arose from the higher sensitivity of the microplate reader than that of ordinary flatbed scanner. The image analysis makes a practical alternative to the absorption analysis, with 100% accuracy in both "leave-one-out" cross-validation and HCA in our study. To the best of our knowledge, this three-unit sensor array is by far the simplest one, which is able to discriminate 15 metal ions at such a low concentration. In addition, to evaluate the robustness of our proposed array, double-blind test was carried out to identify 30 unknown metal ion samples. The results (Table S1†) showed that identification accuracy of 93.33% was achieved, which confirms the feasibility of this sensor array to identify unknown metal ions.

Further exploration of the potential application of this array in quantitative analysis was carried out using both image analysis and absorption analysis. Among these fifteen metal ions, Ni^{2+}, Cu^{2+}, Hg^{2+} (Fig. 3) and Co^{2+} (Fig. S4†) showed good correlations in LDA 2-D figures. As shown in Fig. 3(A, C and E) for Ni^{2+}, Cu^{2+} and Hg^{2+}, the 2-D plots using the first two factors displayed clear separations for different concentrations. Plotting factor 1 (the most significant factor) *vs.* concentrations of these three metal ions showed a good correlation, with the linear detection ranges for Ni^{2+}, Cu^{2+} and Hg^{2+} at 0–4 μM, 0–8 μM and 0.5–3 μM, respectively. The results highly suggest that our proposed sensor array might find its potential application in quantitative analysis of some metal ions. Similar results from absorption spectral data analysis were also obtained with higher sensitivity (Fig. S5†).

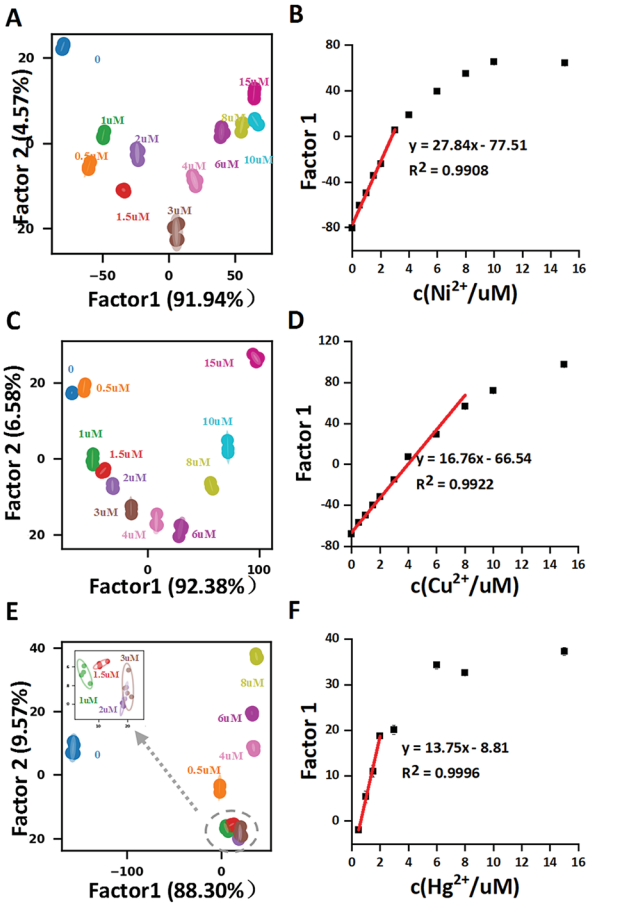

Fig. 3 Discrimination of Ni^{2+}, Cu^{2+} and Hg^{2+} at different concentrations. (A, C and E) LDA plots for the detection of metal ions at different concentrations. (B, D and F) The relationship between factor 1 and different concentrations of metal ions.

Distinguishing mixture samples with different composition of metal ions is a great challenge for sensor arrays. Inspired by the strategy of mixture preparation in Bushdid *et al.* work.[29] We prepared 15 pairs of mixtures (referred to as "mixture A" and "mixture B") that consist of 3, 5 and 7 components drawn from the collection of 15 metal ions (Fig. S6 and Table S2†). To generate each mixture, we combined these components together at equal ratios. The most apparent difference between two pairs of mixtures with the same number of components is the percentage of components they share which varied from 0 to $(N - 1/N)$ (N represents the number of components of the mixture pair). The components in each mixture were randomly selected by a written python program, and the concentration of each component in all mixtures was fixed at 5 μM. Fig. S7† and 4(A, C and E) shows that different pairs displayed distinct colour change patterns, which arose from the different components of the mixtures. LDA 2-D plots demonstrated that all pairs of

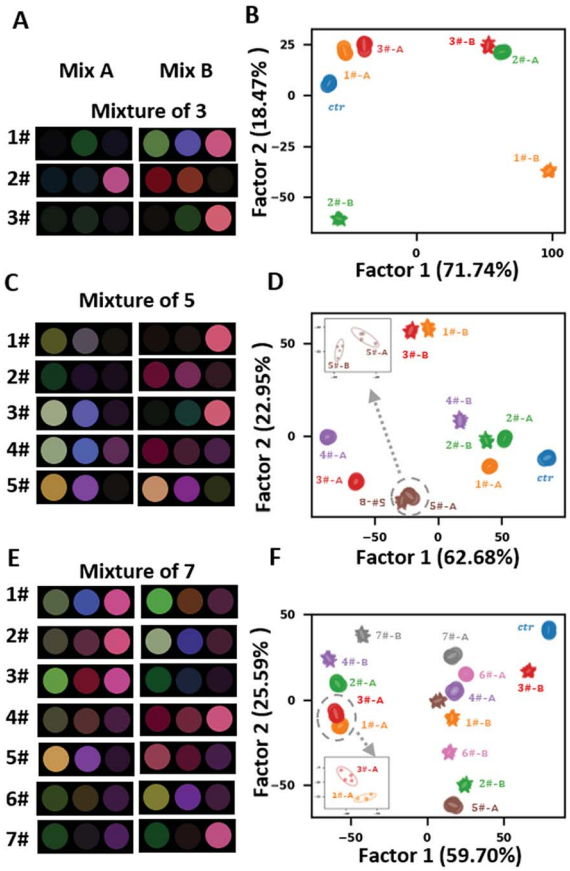

Fig. 4 Colour change profile of mixture A (left) and mixture B (right) of 15 different metal ions mixture pairs including (A) 3 metal ions, (C) 5 metal ions and (E) 7 metal ions. For purposes of visualization, the colour range of the difference map was expanded from 4 to 8 bits per colour (RGB range of 0–77 expanded to 0–255). LDA plot of sensor array against metal ions mixture pairs consists of exactly (B) 3 components, (D) 5 components and (F) 7 components using RGB channels.

mixtures with the same number of components were completely separated (Fig. 4B, E and F). The "leave-one-out" cross-validation reached 100% accuracy and all the samples were clustered correctly in HCA (Fig. S8†). The discrimination capability of image analysis was comparable to that of absorption spectral data analysis (Fig. S9†). These results exhibited the potential of the proposed array as an advanced sensor array which can provide discrimination of highly similar complex mixtures.

Detection of metal ions in real environmental water source are of greater practical significance than lab-prepared samples.

To explore the capacity of our array in practical application, real water samples were tested in our study. 7 real water samples including super pure water (SPW), deionized water (DW), tap water (TW), lake water (LW), artificial lake water (ALW), river water (RW) and sea water (SW) were collected and directly tested without intentionally adding any metal ions. LDA 2-D plot demonstrated that all samples were correctly clustered and completely separated (Fig. 5A), while HCA showed clear discrimination of all real water samples with no misclassification

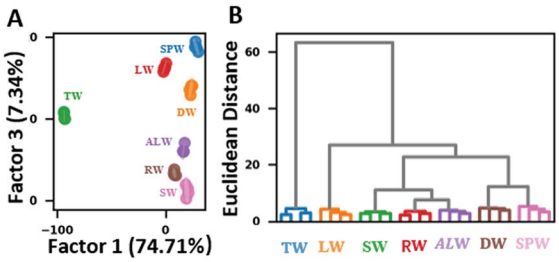

Fig. 5 Performance of the sensor array on distinguishing real water samples. (A) 2D LDA plot and (B) HCA dendrogram using RGB change values.

(Fig. 5B), which was in accordance with the results of absorption spectral data analysis (Fig. S10†). The successful differentiation of real water samples revealed the potential for on-site analysis.

In conclusion, we fabricated a new three-unit colorimetric sensor array using two commercially available low-cost dyes for detection of heavy metal ions in aqueous solution. In addition to commonly used absorption spectral measurements, colorimetric change patterns were also successfully constructed by imaging analysis of RGB values. LDA and HCA results proved that this array could achieve 100% accuracy in discriminating 15 metal ions solutions at 5 μM. Quantitative analysis of several ions was achieved at sub-micromolar range. Mixtures of 3, 5 and 7 metal ions as well as 7 real water samples without additional spiked metal ions were also accurately differentiated by imaging analysis, suggesting that this array has potential for on-site metal ions detection.

Conflicts of interest

There are no conflicts to declare.

Acknowledgements

We acknowledge the financial support from Shenzhen Municipal Government (JCYJ20170817161303009). The authors also acknowledge Ms. Jie Lei's help with python programming.

Notes and references

1 J. R. Askim, M. Mahmoudi and K. S. Suslick, *Chem. Rev.*, 2013, **42**, 8649.
2 Z. Li, J. R. Askim and K. S. Suslick, *Chem. Rev.*, 2019, **119**, 231.
3 M. Zhang, J. J. Sun, M. Khatib, Z. Y. Lin, Z. H. Chen, W. Saliba, A. Gharra, Y. D. Horev, V. Kloper, Y. Milyutin, T. P. Huynh, S. Brandon, G. Y. Shi and H. Haick, *Nat. Commun.*, 2019, **10**, 1120.
4 L. Jia-Wei, H. Chang-Jun, H. Dan-Qun, Y. Mei, Z. Su-Yi, M. Yi and L. Yang, *Anal. Methods*, 2017, **9**, 141.
5 W. Huang, K. Seehafer and U. H. F. Bunz, *ACS Appl. Polym. Mater.*, 2019, **1**, 1301.
6 B. Hemmateenejad, J. Tashkhourian, M. Bordbar and N. Mobaraki, *J. Iran. Chem. Soc.*, 2017, **14**, 595.

7 X. Y. Han, Z. H. Chen, J. Z. Zeng, Q. X. Fan, Z. Q. Fang, G. Y. Shi and M. Zhang, *ACS Appl. Mater. Interfaces*, 2018, **10**, 31725.
8 W. Gao, H. Y. Y. Nyein, Z. Shahpar, H. M. Fahad, K. Chen, S. Emaminejad, Y. J. Gao, L. C. Tai, H. Ota, E. Wu, J. Bullock, Y. P. Zeng, D. H. Lien and A. Javey, *ACS Sens.*, 2016, **1**, 866.
9 Z. Y. Lin, S. F. Xue, Z. H. Chen, X. Y. Han, G. Y. Shi and M. Zhang, *Anal. Chem.*, 2018, **90**, 8248.
10 A. M. Mallet, A. B. Davis, D. R. Davis, J. Panella, K. J. Wallace and M. Bonizzoni, *Chem. Commun.*, 2015, **51**, 16948.
11 Y. Wu, Y. Tan, J. T. Wu, S. Y. Chen, Y. Z. Chen, X. W. Zhou, Y. Y. Jiang and C. Y. Tan, *ACS Appl. Mater. Interfaces*, 2015, **7**, 6882.
12 H. B. Xu, W. Wu, Y. Chen, T. Qiu and L. J. Fan, *ACS Appl. Mater. Interfaces*, 2014, **6**, 5041.
13 W. Xu, C. L. Ren, C. L. Teoh, J. J. Peng, S. H. Gadre, H. W. Rhee, C. L. K. Lee and Y. T. Chang, *Anal. Chem.*, 2014, **86**, 8763.
14 S. F. Xue, Z. H. Chen, X. Y. Han, Z. Y. Lin, Q. X. Wang, M. Zhang and G. Y. Shi, *Anal. Chem.*, 2018, **90**, 3443.
15 J. W. Lee, J. S. Lee, M. Kang, A. I. Su and Y. T. Chang, *Chem. - Eur. J.*, 2006, **12**, 5691.
16 W. W. He, L. Luo, Q. Y. Liu and Z. B. Chen, *Anal. Chem.*, 2018, **90**, 4770.
17 Z. Wang, M. A. Palacios and P. Anzenbacher, *Anal. Chem.*, 2008, **80**, 7451.
18 L. A. Feng, Y. Zhang, L. Y. Wen, L. A. Chen, Z. Shen and Y. F. Guan, *Chem. - Eur. J.*, 2011, **17**, 1101.
19 L. Liu and H. W. Lin, *Anal. Chem.*, 2014, **86**, 8829.
20 N. Idros and D. P. Chu, *ACS Sens.*, 2018, **3**, 1756.
21 S. Abbasi-Moayed, H. Golmohammadi and M. R. Hormozi-Nezhad, *Nanoscale*, 2018, **10**, 2492.
22 H. Fischer and G. Leopoldi, *Mikrochim. Acta*, 1937, **1**, 30.
23 W. E. White, *J. Chem. Educ.*, 1936, **13**, 369.
24 H. J. Wichmann, *Ind. Eng. Chem., Anal. Ed.*, 1939, **11**, 66.
25 H. D. Fiedler, J. L. Westrup, A. J. Souza, A. D. Pavei, C. U. Chagas and F. Nome, *Talanta*, 2004, **64**, 190.
26 Y. M. Leng, S. H. Qian, Y. H. Wang, C. Lu, X. X. Ji, Z. W. Lu and H. W. Lin, *Sci. Rep.*, 2016, **6**, 25354.
27 Y. M. Leng, Y. L. Li, A. Gong, Z. Y. Shen, L. Chen and A. G. Wu, *Langmuir*, 2013, **29**, 7591.
28 E. Y. Arslan and S. Cakir, *S. Afr. J. Chem.*, 2010, **63**, 152.
29 C. Bushdid, M. O. Magnasco, L. B. Vosshall and A. Keller, *Science*, 2014, **343**, 1370.